

# Incremental Collision Laws Based on the Bouc-Wen Model: External Forces and Corner Cases

**Mihails Milehins<sup>1</sup>**

Department of Mechanical Engineering,  
Auburn University,  
Auburn, AL 36849,  
email: mzm0390@auburn.edu

**Dan B. Marghitu**

Department of Mechanical Engineering,  
Auburn University,  
Auburn, AL 36849,  
email: marghdb@auburn.edu

*In the article titled “The Bouc–Wen Model for Binary Direct Collinear Collisions of Convex Viscoplastic Bodies” and published in the Journal of Computational and Nonlinear Dynamics, the authors studied mathematical models of binary direct collinear collisions of convex viscoplastic bodies that employed two incremental collision laws based on the Bouc–Wen differential model of hysteresis. It was shown that the models possess favorable analytical properties, and several model parameter identification studies were conducted in an attempt to validate the models. In this article, these models are augmented by taking into account the effects of external forces that are modeled as time-dependent inputs that belong to a certain function space. Furthermore, the range of the parameters under which the models possess favorable analytical properties is extended to several corner cases that were not considered in the prior publication. Finally, the previously conducted model parameter identification studies are extended, and an additional model parameter identification study is provided in an attempt to validate the ability of the augmented models to represent the effects of external forces.*

**Keywords:** Impact and Contact Modeling, Multibody System Dynamics, Nonlinear Dynamical Systems

## 1 Introduction

There exist two primary approaches for modeling of systems of rigid bodies with contacts: nonsmooth dynamics formulations (e.g., see Refs. [1–6]) and continuous formulations (e.g., see Refs. [7–10]). This article is concerned with continuous formulations, which require a dynamic model that can describe the evolution of the contact force during the collision events (e.g., see Refs. [11, 12]). Such dynamic models are referred to as incremental collision laws.

In Ref. [13], the authors studied mathematical models of binary direct collinear collisions of convex viscoplastic bodies using two incremental collision laws based on the Bouc-Wen differential hysteresis model ([14–16], see also Ref. [17]). These collision laws are the Bouc-Wen-Simon-Hunt-Crossley Collision Law (BWSHCCL) and the Bouc-Wen-Maxwell Collision Law (BWMCL). They were designed based on the ideas underpinning the Simon-Hunt-Crossley Collision Law (see Ref. [Simon (1967), as cited in Ref. 5] and Ref. [18]), and the Maxwell Collision Law (see Refs. [19–21]), respectively. The BWSHCCL was stated as<sup>2</sup>

$$\begin{cases} \dot{x} = u \\ \dot{z} = Au - \beta|z|^{n-1}z|u| - \gamma|z|^n u \\ F = -\alpha k|x|^{p-1}x - \alpha_c k|z|^{p-1}z - c|x|^p u \end{cases} \quad (1)$$

where  $x \in \mathbb{R}$  is a state variable that represents the relative displacement of the colliding bodies,  $z \in \mathbb{R}$  is a state variable that represents the hysteretic displacement of the colliding bodies,  $u \in \mathbb{R}$  is an input variable that is meant to represent the relative velocity of the colliding bodies,  $F \in \mathbb{R}$  is an output variable that is meant to represent the contact force between the colliding bodies; the model was parameterized by  $A, k \in \mathbb{R}_{>0}$ ,  $\alpha \in (0, 1)$ ,  $c, \beta \in \mathbb{R}_{\geq 0}$ ,  $\gamma \in [-\beta, \beta]$ ,

and  $n \in \mathbb{R}_{\geq 1}$ , with  $\alpha_c \triangleq 1 - \alpha$ .<sup>3</sup> The BWMCL was stated as

$$\begin{cases} \dot{r} = \alpha \frac{k}{c}|y|^{p-1}y + \alpha_c \frac{k}{c}|z|^{p-1}z \\ \dot{y} = -\dot{r} + u \\ \dot{z} = A\dot{y} - \beta|z|^{n-1}z|\dot{y}| - \gamma|z|^n \dot{y} \\ F = -c\dot{r} = -\alpha k|y|^{p-1}y - \alpha_c k|z|^{p-1}z \end{cases} \quad (2)$$

where  $r \in \mathbb{R}$  is a state variable that represents the relative displacement of the linear viscous dissipation element,  $y \in \mathbb{R}$  is a state variable that represents the relative displacement of the Bouc-Wen hysteretic element,  $z \in \mathbb{R}$  is a state variable that represents the hysteretic displacement in the Bouc-Wen hysteretic element,  $u \in \mathbb{R}$  is an input variable that is meant to represent the relative velocity of the colliding bodies,  $F \in \mathbb{R}$  is an output variable that is meant to represent the contact force between the colliding bodies; the model is parameterized by  $A, k, c \in \mathbb{R}_{>0}$ ,  $\alpha \in (0, 1)$ ,  $\beta \in \mathbb{R}_{\geq 0}$ ,  $\gamma \in [-\beta, \beta]$ , and  $n \in \mathbb{R}_{\geq 1}$ .

The Bouc-Wen-Simon-Hunt-Crossley Collision Model (BWSHCCM) which is meant to represent binary direct collinear collisions and employs the BWSHCCL to model the contact force at the interface between the bodies was stated as

$$\begin{cases} \dot{x} = v \\ \dot{z} = Av - \beta|z|^{n-1}z|v| - \gamma|z|^n v \\ \dot{v} = -\alpha \frac{k}{m}|x|^{p-1}x - \alpha_c \frac{k}{m}|z|^{p-1}z - \frac{c}{m}|x|^p v \\ x(0) = 0, \quad z(0) = 0, \quad v(0) = -v_0 \end{cases} \quad (3)$$

where  $x \in \mathbb{R}$  is a state variable that represents the relative displacement of the bodies during the collision,  $z$  is a state variable that represents the hysteretic displacement associated with the BWSHCCL,  $v \in \mathbb{R}$  is a state variable that represents the relative velocity of the bodies during the collision,  $m \in \mathbb{R}_{>0}$  is a parameter that represents the effective mass of the colliding bodies (an explanation is provided in Section 2),  $v_0 \in \mathbb{R}_{>0}$  is a parameter that describes the initial relative velocity of the bodies (i.e., the relative velocity of

<sup>1</sup>Corresponding Author.

July 11, 2025

<sup>2</sup>The conventions are adopted from Ref. [13], and will not be restated for the sake of brevity. However, the conventions that are specific to the present study are provided in Appendix B.

<sup>3</sup>In what follows,  $\alpha_c$  will always be used as an abbreviation for  $1 - \alpha$ .

the bodies immediately prior to the collision), other parameters are adopted from the BWSHCCCL.

The Bouc-Wen-Maxwell Collision Model (BWMCM) was stated as

$$\begin{cases} \dot{r} = \alpha \frac{k}{c} |y|^{p-1} y + \alpha_c \frac{k}{c} |z|^{p-1} z \\ \dot{y} = w \\ \dot{z} = Aw - \beta |z|^{n-1} z |w| - \gamma |z|^n w \\ \dot{w} = -\frac{c}{m} \dot{r} - \alpha p \frac{k}{c} |y|^{p-1} \dot{y} - \alpha_c p \frac{k}{c} |z|^{p-1} \dot{z} \\ r(0) = y(0) = z(0) = 0, \quad w(0) = -v_0 \end{cases} \quad (4)$$

where  $r \in \mathbb{R}$  is a state variable that represents the relative displacement of the linear viscous energy dissipation element associated with the BWMCL,  $y \in \mathbb{R}$  is a relative displacement of the Bouc-Wen hysteretic element associated with the BWMCL,  $z \in \mathbb{R}$  is the hysteretic displacement of the Bouc-Wen hysteretic element associated with the BWMCL,  $w \in \mathbb{R}$  is a state variable that represents the relative velocity of the Bouc-Wen hysteretic element associated with the BWMCL,  $m \in \mathbb{R}_{>0}$  is a parameter that represents the effective mass of the colliding bodies (an explanation is provided in Section 2),  $v_0 \in \mathbb{R}_{>0}$  is a parameter that describes the initial relative velocity of the bodies, other parameters are adopted from the BWMCL. The relative displacement  $x$  and the relative velocity  $v$  can be recovered by augmenting the BWMCM with the output function given by

$$\begin{cases} x = r + y \\ v = \dot{r} + \dot{y} \end{cases} \quad (5)$$

or, alternatively, with the state variables  $x$  and  $v$  constrained via

$$\begin{cases} \dot{x} = v \\ \dot{v} = -\frac{c}{m} \dot{r} \\ x(0) = 0, \quad v(0) = -v_0 \end{cases} \quad (6)$$

The nondimensionalized form of the BWSHCCM, referred to as the Nondimensionalized Bouc-Wen-Simon-Hunt-Crossley Collision Model (NDBWSHCCM), was given by

$$\begin{cases} \dot{X} = V \\ \dot{Z} = V - B|Z|^{n-1}Z|V| - \Gamma|Z|^nV \\ \dot{V} = -\kappa|X|^{p-1}X - \kappa_c|Z|^{p-1}Z - \sigma|X|^pV \\ X(0) = 0, \quad Z(0) = 0, \quad V(0) = -1 \end{cases} \quad (7)$$

The relationships between the nondimensionalized and dimensional variables were given by  $T \triangleq t/T_c$ ,  $X \triangleq x/X_c$ ,  $Z \triangleq z/Z_c$ ,  $V \triangleq v/(X_c/T_c)$ . The parameters that were used for the nondimensionalization are given in Table 1.

The nondimensionalized form of the BWMCM, referred to as the Nondimensionalized Bouc-Wen-Maxwell Collision Model (NDBWMCM), was given by

$$\begin{cases} \dot{R} = \kappa\sigma|Y|^{p-1}Y + \kappa_c\sigma|Z|^{p-1}Z \\ \dot{Y} = W \\ \dot{Z} = W - B|Z|^{n-1}Z|W| - \Gamma|Z|^nW \\ \dot{W} = -\frac{1}{\sigma}\dot{R} - \kappa p\sigma|Y|^{p-1}\dot{Y} - \kappa_c p\sigma|Z|^{p-1}\dot{Z} \\ R(0) = Y(0) = Z(0) = 0, \quad W(0) = -1 \end{cases} \quad (8)$$

As previously, it can be augmented by the output function

$$\begin{cases} X = R + Y \\ V = \dot{R} + \dot{Y} \end{cases} \quad (9)$$

or the additional states  $X$  and  $V$  constrained via

$$\begin{cases} \dot{X} = V \\ \dot{V} = -\frac{1}{\sigma}\dot{R} \\ X(0) = 0, \quad V(0) = -1 \end{cases} \quad (10)$$

The relationships between the nondimensionalized and dimensional variables were given by  $T \triangleq t/T_c$ ,  $R \triangleq r/X_c$ ,  $Y \triangleq y/X_c$ ,  $Z \triangleq z/Z_c$ ,  $W \triangleq w/(X_c/T_c)$ ,  $X \triangleq x/X_c$ ,  $V \triangleq v/(X_c/T_c)$ . The parameters that were used for nondimensionalization are given in Table 1.

In Ref. [13], the authors show that if the NDBWSHCCM is parameterized by  $B \in \mathbb{R}_{\geq 0}$ ,  $\Gamma \in [-B, B]$ ,  $\kappa \in (0, 1)$ ,  $\sigma \in \mathbb{R}_{\geq 0}$ ,  $n, p \in \mathbb{R}_{\geq 1}$ , then the NDBWSHCCM has a unique bounded solution on any time interval  $[0, T_e)$  with  $T_e \in \mathbb{R}_{>0} \cup \{+\infty\}$ . The authors also show that if the NDBWMCM is parameterized by  $B \in \mathbb{R}_{>0}$ ,  $\Gamma \in (-B, B)$ ,  $\kappa \in (0, 1)$ ,  $\sigma \in \mathbb{R}_{>0}$ ,  $n \in \mathbb{R}_{\geq 1}$ ,  $p \in \mathbb{R}_{\geq 2} \cup \{1\}$ , then the NDBWMCM has a unique bounded solution on any time interval  $[0, T_e)$  with  $T_e \in \mathbb{R}_{>0} \cup \{+\infty\}$ . Moreover, the output associated with this solution is bounded. Furthermore, the authors show that (under a slightly more restricted set of parameters) the solutions of the NDBWSHCCM and the NDBWMCM converge to an infinite set of equilibrium points at a finite distance from the origin. Lastly, the authors conduct two model parameter identification studies that demonstrate that both the NDBWSHCCM and the NDBWMCM can accurately represent a variety of collision phenomena.

While the authors of Ref. [13] performed a substantial amount of work on the analysis and validation of the NDBWSHCCM and the NDBWMCM, there is still potential scope for improvement of the models and the associated analytical framework:

- Both the BWSHCCM and the BWMCM were designed under the assumption that the only force that is acting on the bodies during the collision is the contact force. This idealization can often serve as a good approximation. However, in some cases, the external forces that are acting on the bodies during the collision process cannot be ignored (e.g., see Refs. [22–30]).
- The authors do not provide analysis of the NDBWMCM for the following choices of parameters:  $B = 0$ ,  $\Gamma \in \{-B, B\}$ ,  $p \in (1, 2)$ . These parameters lie within the physically plausible range and, therefore, may be important for applications.
- The authors provided no explanation for why the force of gravity could be ignored during the identification of the models based on the experimental data provided in Ref. [31]. Furthermore, the identification of the parameters of the NDBWMCM based on the dataset provided in Fig. 1 in Ref. [31] was performed under the assumption that  $p \in (1, 2)$ .
- The parameter identification study based on the dataset in Fig. 9.5 in Ref. [32] was restricted to the BWSHCCM, and no comments were provided with regard to whether the BWMCM is a suitable model for the description of the physical phenomenon analyzed in Ref. [32].

It is the goal of the present article to resolve the issues outlined in the list above. Thus, the BWSHCCM and the BWMCM will be augmented with the action of external forces (albeit under certain convenient restrictions), and the analysis of the models will be updated to include the aforementioned corner cases.<sup>4</sup> Furthermore, the model parameter identification studies will be updated in an attempt to close the gaps mentioned above. Lastly, a further model parameter identification study will be provided in an attempt to validate the BWSHCCM and the BWMCM augmented with the action of external forces.

## 2 Model of the Physical System

It is assumed that  $\mathcal{B}_1$  is a compact and strictly convex rigid body and  $\mathcal{B}_2$  is a convex rigid body with a topologically smooth surface. The bodies are assumed to come into contact (at a single point) at the time  $t_0 \in \mathbb{R}_{\geq 0}$  with their centers of mass lying on a line that passes through the point of contact. The velocity fields of both bodies are assumed to be uniform and parallel to this

<sup>4</sup>It should be noted that the analysis of the long-term behavior of the solutions was not repeated in the present study, as it has limited value in the context of analysis of (largely) finite-time collision phenomena.

**Table 1** Parameters for nondimensionalization

Parameters	BWSHCCM	BWMCM
$T_c$	$\left(\frac{1}{\alpha + \alpha_c A^p}\right)^{\frac{1}{p+1}} \left(\frac{m}{k}\right)^{\frac{1}{p+1}} v_0^{-\frac{p-1}{p+1}}$	$\left(\frac{1}{\alpha + \alpha_c A^p}\right)^{\frac{1}{p+1}} \left(\frac{m}{k}\right)^{\frac{1}{p+1}} v_0^{-\frac{p-1}{p+1}}$
$X_c$	$\left(\frac{1}{\alpha + \alpha_c A^p}\right)^{\frac{1}{p+1}} \left(\frac{m}{k}\right)^{\frac{1}{p+1}} v_0^{\frac{2}{p+1}}$	$\left(\frac{1}{\alpha + \alpha_c A^p}\right)^{\frac{1}{p+1}} \left(\frac{m}{k}\right)^{\frac{1}{p+1}} v_0^{\frac{2}{p+1}}$
$Z_c$	$\left(\frac{1}{\alpha + \alpha_c A^p}\right)^{\frac{1}{p+1}} A \left(\frac{m}{k}\right)^{\frac{1}{p+1}} v_0^{\frac{2}{p+1}}$	$\left(\frac{1}{\alpha + \alpha_c A^p}\right)^{\frac{1}{p+1}} A \left(\frac{m}{k}\right)^{\frac{1}{p+1}} v_0^{\frac{2}{p+1}}$
$B$	$\left(\frac{A^{p+1}}{\alpha + \alpha_c A^p}\right)^{\frac{n}{p+1}} \frac{\beta}{A} \left(\frac{m}{k}\right)^{\frac{n}{p+1}} v_0^{\frac{2n}{p+1}}$	$\left(\frac{A^{p+1}}{\alpha + \alpha_c A^p}\right)^{\frac{n}{p+1}} \frac{\beta}{A} \left(\frac{m}{k}\right)^{\frac{n}{p+1}} v_0^{\frac{2n}{p+1}}$
$\Gamma$	$\left(\frac{A^{p+1}}{\alpha + \alpha_c A^p}\right)^{\frac{n}{p+1}} \frac{\gamma}{A} \left(\frac{m}{k}\right)^{\frac{n}{p+1}} v_0^{\frac{2n}{p+1}}$	$\left(\frac{A^{p+1}}{\alpha + \alpha_c A^p}\right)^{\frac{n}{p+1}} \frac{\gamma}{A} \left(\frac{m}{k}\right)^{\frac{n}{p+1}} v_0^{\frac{2n}{p+1}}$
$\kappa$	$\frac{\alpha}{\alpha + \alpha_c A^p}$	$\frac{\alpha}{\alpha + \alpha_c A^p}$
$\sigma$	$\frac{1}{\alpha + \alpha_c A^p} \frac{c}{k} v_0$	$(\alpha + \alpha_c A^p)^{\frac{1}{p+1}} \frac{1}{c} (m^p k)^{\frac{1}{p+1}} v_0^{\frac{p-1}{p+1}}$

line. The configuration, as hereinbefore described, corresponds to a binary direct collinear impact (e.g., see Ref. [33]). Following the methodology proposed in Ref. [33], it shall be assumed that while the bodies remain in contact, the motion of the system is governed by the laws of rigid body dynamics (Newton, [34]), with the contact point described as an infinitesimal deformable particle. In this case, only one generalized coordinate is sufficient to describe the motion of each body. The model of the bodies during contact can be expressed as<sup>5</sup>

$$\begin{cases} \ddot{x}_1 = m_1^{-1} F + m_1^{-1} u_1 \\ \ddot{x}_2 = -m_2^{-1} F + m_2^{-1} u_2 \\ x_1(t_0) = x_2(t_0) = 0, \quad \dot{x}_1(t_0) = v_{1,0}, \quad \dot{x}_2(t_0) = v_{2,0} \end{cases} \quad (11)$$

where  $t_0 \in \mathbb{R}_{\geq 0}$ , and for each  $i \in \{1, 2\}$ ,<sup>6</sup>  $x_i \in \mathbb{R}$  is a state variable that describes the location of the center of mass of  $\mathcal{B}_i$  relative to the initial location of the center of mass of  $\mathcal{B}_i$  at the time of the collision,  $m_i$  is a parameter that describes the mass of  $\mathcal{B}_i$ ,  $u_i : \mathbb{R}_{\geq 0} \rightarrow \mathbb{R}$  is a function that represents an external force that is acting on  $\mathcal{B}_i$  in a direction parallel to the direction of motion,  $v_{i,0} \in \mathbb{R}$  is the velocity of  $\mathcal{B}_i$  at the time of the collision. It is assumed that  $u_i$  is continuous and  $\|u_i\|_1 \triangleq \int_0^{+\infty} |u_i(s)| ds < +\infty$ .<sup>7</sup> The space of all such functions shall be denoted as  $\mathcal{U}_1$ . It is also assumed that the parameters  $v_{1,0}$  and  $v_{2,0}$  are constrained via  $v_0 \triangleq -(v_{1,0} - v_{2,0}) \in \mathbb{R}_{>0}$ . Denoting

$$m \triangleq \frac{m_1 m_2}{m_1 + m_2} \in \mathbb{R}_{>0} \quad (12)$$

$$u \triangleq \frac{u_1 m_2 - u_2 m_1}{m_1 + m_2} : \mathbb{R}_{\geq 0} \rightarrow \mathbb{R} \quad (13)$$

$$x \triangleq x_1 - x_2 \quad (14)$$

$$v \triangleq \dot{x} = \dot{x}_1 - \dot{x}_2 \quad (15)$$

the equations of motion can be transformed to

$$\begin{cases} \dot{x} = v & x(t_0) = 0 \\ \dot{v} = m^{-1} F + m^{-1} u & v(t_0) = -v_0 \end{cases} \quad (16)$$

The form of the force  $F$  depends on the chosen collision law. It should be noted that if (by abuse of notation)  $m_2 = +\infty$ , then

<sup>5</sup>A more detailed explanation of the model and the methodology that was used for its derivation can be found in Ref. [13].

<sup>6</sup>In what follows, it shall always be assumed that  $i$  ranges over the set  $\{1, 2\}$ .

<sup>7</sup>Since for the majority of applications only finite-time impacts are of interest, the regularity conditions that are imposed on  $u_i$  are hardly restrictive. Nonetheless, lifting these restrictions may offer useful analytical insight.

$m^{-1} = m_1^{-1}$  and  $u = u_1$ . This situation corresponds to the collision of a body  $\mathcal{B}_1$  of finite mass with a stationary body  $\mathcal{B}_2$ .

Assuming existence and uniqueness of a solution of the IVP given by Eq. (16) on some non-degenerate time interval  $I \subseteq \mathbb{R}_{\geq 0}$  with  $t_0 \in I$ , the time of the separation  $t_s \in \mathbb{R}_{> t_0} \cup \{+\infty\}$  is defined as

$$t_s \triangleq \inf\{t \in I_{\geq t_0} : F(t) \leq 0 \wedge 0 \leq v(t)\} \quad (17)$$

and the Kinetic Coefficient of Restitution (CoR)  $e \in \mathbb{R}$  as<sup>8</sup>

$$e \triangleq \begin{cases} -v(t_s)/v(t_0) & t_s \neq +\infty \\ 0 & t_s = +\infty \end{cases} \quad (18)$$

It should be remarked that the effects of the external force are ignored in the definition of the time of the separation (cf. [24]).

### 3 The Bouc-Wen-Simon-Hunt-Crossley Collision Model

Taking into account the modifications of the model of the physical system in Eq. (16), the BWSHCCM can be stated as<sup>9</sup>

$$\begin{cases} \dot{x} = v \\ \dot{z} = A v - \beta |z|^{n-1} |z| v - \gamma |z|^n v \\ \dot{v} = -\alpha \frac{k}{m} |x|^{p-1} x - \alpha_c \frac{k}{m} |z|^{p-1} z - \frac{c}{m} |x|^p v + \frac{1}{m} u \\ x(t_0) = 0, \quad z(t_0) = 0, \quad v(t_0) = -v_0 \end{cases} \quad (19)$$

Introduction of the variable  $T_0 \in \mathbb{R}_{\geq 0}$  given by  $T_0 \triangleq t_0/T_c$  (with  $T_c$  given in Table 1), the function  $U : \mathbb{R}_{\geq 0} \rightarrow \mathbb{R}$  given by

$$U \triangleq \left(\frac{1}{\alpha + \alpha_c A^p}\right)^{\frac{1}{p+1}} (m^p k)^{-\frac{1}{p+1}} v_0^{-\frac{2p}{p+1}} u \quad (20)$$

and nondimensionalization of the BWSHCCM using the methodology presented in Ref. [35] and the parameters listed in Table 1 results in the new form of the NDBWSHCCM:

$$\begin{cases} \dot{X} = V \\ \dot{Z} = V - B |Z|^{n-1} |Z| V - \Gamma |Z|^n V \\ \dot{V} = -\kappa |X|^{p-1} X - \kappa_c |Z|^{p-1} Z - \sigma |X|^p V + U \\ X(T_0) = 0, \quad Z(T_0) = 0, \quad V(T_0) = -1 \end{cases} \quad (21)$$

It should be remarked that since  $u_i$  are in  $\mathcal{U}_1$  for both admissible  $i$ ,  $U$  is also in  $\mathcal{U}_1$ .

<sup>8</sup>See [33] for a conceptual description of the kinetic coefficient of restitution, which is usually attributed to Sir Isaac Newton [34], and for other types of coefficients of restitution.

<sup>9</sup>The naming conventions will be preserved despite the introduction of external forces.

Under the assumption that  $B \in \mathbb{R}_{\geq 0}$ ,  $\Gamma \in [-B, B]$ ,  $\kappa \in (0, 1)$ ,  $\sigma \in \mathbb{R}_{\geq 0}$ ,  $n, p \in \mathbb{R}_{\geq 1}$ , the NDBWSHCCM has unique bounded solutions forward in time that can be extended to infinity. The details of the analysis that led to these conclusions are presented in Appendix B.

In Ref. [13], the authors provide a relationship that describes the dependence of the parameters of the NDBWSHCCM on  $v_0$ , which can be useful for applications (see Section 5). Taking under consideration the updates that were made to the NDBWSHCCM, and assuming that the input  $u \in \mathcal{U}_1$  that represents the external forces is fixed and known, the relationship can be described by the function  $\mathcal{P} : \mathbb{P}^* \times \mathbb{R}_{>0} \rightarrow \mathbb{P} \times \mathcal{U}_1$  that maps  $(B_b, \Gamma_b, \kappa, \sigma_b, n, p, U_b) \in \mathbb{P}^*$  and  $v_0 \in \mathbb{R}_{>0}$  to

$$\left( B_b v_0^{\frac{2n}{p+1}}, \Gamma_b v_0^{\frac{2n}{p+1}}, \kappa, \sigma_b v_0, n, p, U_b v_0^{-\frac{2p}{p+1}} u \right) \in \mathbb{P} \times \mathcal{U}_1$$

where  $\mathbb{P}^* \subseteq \mathbb{R}^7$  consist of all  $P^* = (B_b, \Gamma_b, \kappa, \sigma_b, n, p, U_b)$  such that  $B_b \in \mathbb{R}_{\geq 0}$ ,  $\Gamma_b \in [-B_b, B_b]$ ,  $\kappa \in (0, 1)$ ,  $\sigma_b \in \mathbb{R}_{\geq 0}$ ,  $n, p \in \mathbb{R}_{\geq 1}$ ,  $U_b \in \mathbb{R}_{>0}$ , and  $\mathbb{P} \subseteq \mathbb{R}^6$  consists of all admissible parameters  $P = (B, \Gamma, \kappa, \sigma, n, p)$  of the NDBWSHCCM. The members of  $\mathbb{P}^*$  are referred to as the base parameters: they are merely convenient abstractions for the study of the behavior of a given physical system represented by the NDBWSHCCM with respect to the changes in the initial relative velocity (e.g., see Section 5). Thus,  $\mathcal{P}$  maps the base parameters to the admissible parameters and the admissible inputs of the NDBWSHCCM.

The functions that represent the relationship between the parameters and the observables of interest are also updated. Thus,  $\Phi : \mathbb{P} \times \mathcal{U}_1 \times \mathbb{R}_{\geq T_0} \rightarrow \mathbb{R}^3$  is defined to be such that  $\Phi_{P,U}(T)$  represents the value of the solution of the NDBWSHCCM parameterized by  $P \in \mathbb{P}$  and the input  $U \in \mathcal{U}_1$  at the time  $T \in \mathbb{R}_{\geq T_0}$ ; the contact force  $F : \mathbb{P} \times \mathbb{R}^3 \rightarrow \mathbb{R}$  for the NDBWSHCCM shall be defined as

$$F_P(X, Z, V) \triangleq -\kappa|X|^{p-1}X - \kappa_c|Z|^{p-1}Z - \sigma|X|^pV \quad (22)$$

for any  $(X, Z, V) \in \mathbb{R}^3$  and  $P \in \mathbb{P}$  such that  $\kappa = P_3$ ,  $\sigma = P_4$ , and  $p = P_6$ ; the time of the separation  $T_s : \mathbb{P} \times \mathcal{U}_1 \rightarrow \mathbb{R}_{>T_0} \cup \{+\infty\}$  for the NDBWSHCCM shall be defined as

$$T_s(P, U) \triangleq \inf\{T \in \mathbb{R}_{\geq T_0} : F_P(\Phi_{P,U}(T)) \leq 0 \wedge 0 \leq \Phi_{P,U,3}(T)\} \quad (23)$$

for all  $P \in \mathbb{P}$  and  $U \in \mathcal{U}_1$ ; CoR  $e : \mathbb{P} \times \mathcal{U}_1 \rightarrow \mathbb{R}$  for the NDBWSHCCM shall be defined as

$$e(P, U) \triangleq \begin{cases} \Phi_{P,U,3}(T_s(P, U)) & T_s(P, U) \neq +\infty \\ 0 & T_s(P, U) = +\infty \end{cases} \quad (24)$$

for all  $P \in \mathbb{P}$  and  $U \in \mathcal{U}_1$ .

#### 4 The Bouc-Wen-Maxwell Collision Model

Taking into account the modifications of the model of the physical system in Eq. (16), the BWCM can be stated as

$$\begin{cases} \dot{r} = \alpha \frac{k}{c} |y|^{p-1} y + \alpha_c \frac{k}{c} |z|^{p-1} z \\ \dot{y} = -\alpha \frac{k}{c} |y|^{p-1} y - \alpha_c \frac{k}{c} |z|^{p-1} z + v \\ \dot{z} = A\dot{y} - \beta |z|^{n-1} z |\dot{y}| - \gamma |z|^n \dot{y} \\ \dot{x} = v \\ \dot{v} = -\alpha \frac{k}{m} |y|^{p-1} y - \alpha_c \frac{k}{m} |z|^{p-1} z + \frac{1}{m} u \\ r(t_0) = y(t_0) = z(t_0) = x(t_0) = 0, \quad v(t_0) = -v_0 \end{cases} \quad (25)$$

It should be noted that the form of the model BWCM given by Eq. (25) differs from the form of the model that was employed in Ref. [13] and given by Eq. (4) and Eq. (5) or Eq. (6). However, these two forms are equivalent. That is, the model given by Eq.

(4) and Eq. (5) or Eq. (6), and the model given by Eq. (25) yield identical solutions under the assumption that

$$w = -\alpha \frac{k}{c} |y|^{p-1} y - \alpha_c \frac{k}{c} |z|^{p-1} z + v \quad (26)$$

is one of the outputs of the model given by Eq. (25), and provided that the effects of external forces are ignored in Eq. (25) ( $u = 0$ ). The details of the analysis that led to this conclusion are presented in Appendix C. The primary advantage of the form of the model given by Eq. (25) is that the state function associated with the model is locally Lipschitz continuous. This guarantees uniqueness (and local existence) of the solutions of both models. However, it is more difficult to show uniqueness of the solutions directly for the model given by Eq. (5).<sup>10</sup>

Introduction of the variable  $T_0 \in \mathbb{R}_{\geq 0}$  given by  $T_0 \triangleq t_0/T_c$  (with  $T_c$  given in Table 1), the function  $U : \mathbb{R}_{\geq 0} \rightarrow \mathbb{R}$  given by

$$U \triangleq \left( \frac{1}{\alpha + \alpha_c A p} \right)^{\frac{1}{p+1}} (m^p k)^{-\frac{1}{p+1}} v_0^{-\frac{2p}{p+1}} u \quad (27)$$

and nondimensionalization of the BWCM using the methodology presented in Ref. [35] and the parameters listed in Table 1 results in the new form of the NDBWMCM:

$$\begin{cases} \dot{R} = \kappa \sigma |Y|^{p-1} Y + \kappa_c \sigma |Z|^{p-1} Z \\ \dot{Y} = -\kappa \sigma |Y|^{p-1} Y - \kappa_c \sigma |Z|^{p-1} Z + V \\ \dot{Z} = \dot{Y} - B |Z|^{n-1} Z |\dot{Y}| - \Gamma |Z|^n \dot{Y} \\ \dot{X} = V \\ \dot{V} = -\kappa |Y|^{p-1} Y - \kappa_c |Z|^{p-1} Z + U \\ R(T_0) = Y(T_0) = Z(T_0) = X(T_0) = 0, \quad V(T_0) = -1 \end{cases} \quad (28)$$

It should be remarked that since  $u_i$  are in  $\mathcal{U}_1$  for both admissible  $i$ ,  $U$  is also in  $\mathcal{U}_1$ .

Under the assumption that  $B \in \mathbb{R}_{\geq 0}$ ,  $\Gamma \in [-B, B]$ ,  $\kappa \in (0, 1)$ ,  $\sigma \in \mathbb{R}_{>0}$ ,  $n, p \in \mathbb{R}_{\geq 1}$ , the NDBWMCM has unique bounded solutions forward in time that can be extended to infinity. The details of the analysis that led to this conclusion are presented in Appendix C.

Like in Section 3, the description of the dependence of the parameters of the NDBWMCM on  $v_0$  will now be updated. Assuming that the input  $u \in \mathcal{U}_1$  that represents the external forces is fixed and known, the relationship is described by the function  $\mathcal{P} : \mathbb{P}^* \times \mathbb{R}_{>0} \rightarrow \mathbb{P} \times \mathcal{U}_1$  that maps  $(B_b, \Gamma_b, \kappa, \sigma_b, n, p, U_b) \in \mathbb{P}^*$  and  $v_0 \in \mathbb{R}_{>0}$  to

$$\left( B_b v_0^{\frac{2n}{p+1}}, \Gamma_b v_0^{\frac{2n}{p+1}}, \kappa, \sigma_b v_0^{\frac{p-1}{p+1}}, n, p, U_b v_0^{-\frac{2p}{p+1}} u \right) \in \mathbb{P} \times \mathcal{U}_1$$

where  $\mathbb{P}^* \subseteq \mathbb{R}^7$  consist of all  $P^* = (B_b, \Gamma_b, \kappa, \sigma_b, n, p, U_b)$  such that  $B_b \in \mathbb{R}_{\geq 0}$ ,  $\Gamma_b \in [-B_b, B_b]$ ,  $\kappa \in (0, 1)$ ,  $\sigma_b \in \mathbb{R}_{>0}$ ,  $n, p \in \mathbb{R}_{\geq 1}$ ,  $U_b \in \mathbb{R}_{>0}$ , and  $\mathbb{P} \subseteq \mathbb{R}^6$  consists of all admissible parameters  $P = (B, \Gamma, \kappa, \sigma, n, p)$  of the NDBWMCM. Furthermore,  $\Phi : \mathbb{P} \times \mathcal{U}_1 \times \mathbb{R}_{\geq T_0} \rightarrow \mathbb{R}^5$  is defined to be such that  $\Phi_{P,U}(T)$  represents the value of the solution of the NDBWMCM parameterized by  $P \in \mathbb{P}$  and the input  $U \in \mathcal{U}_1$  at the time  $T \in \mathbb{R}_{\geq T_0}$ ; the contact force  $F : \mathbb{P} \times \mathbb{R}^5 \rightarrow \mathbb{R}$  for the NDBWMCM shall be defined as

$$F_P(R, Y, Z, X, V) \triangleq -\kappa |Y|^{p-1} Y - \kappa_c |Z|^{p-1} Z \quad (29)$$

for any  $(R, Y, Z, X, V) \in \mathbb{R}^5$  and  $P \in \mathbb{P}$  such that  $\kappa = P_3$  and  $p = P_6$ ; the time of the separation  $T_s : \mathbb{P} \times \mathcal{U}_1 \rightarrow \mathbb{R}_{>T_0} \cup \{+\infty\}$  for the NDBWMCM shall be defined as

$$T_s(P) \triangleq \inf\{T \in \mathbb{R}_{\geq T_0} : F_P(\Phi_{P,U}(T)) \leq 0 \wedge 0 \leq \Phi_{P,U,5}(T)\} \quad (30)$$

<sup>10</sup>The choice of the form of the model in Ref. [13] was, perhaps, an oversight on behalf of the authors, albeit it may possess certain advantages over the form of the model proposed in this article (its state function has fewer terms, and not more than one term under the absolute value operator).



for all  $P \in \mathbb{P}$  and  $U \in \mathcal{U}_1$ ; CoR  $e : \mathbb{P} \times \mathcal{U}_1 \rightarrow \mathbb{R}$  for the NDBWSHCCM shall be defined as

$$e(P, U) \triangleq \begin{cases} \Phi_{P,U,5}(T_s(P, U)) & T_s(P, U) \neq +\infty \\ 0 & T_s(P, U) = +\infty \end{cases} \quad (31)$$

for all  $P \in \mathbb{P}$  and  $U \in \mathcal{U}_1$ .

## 5 Model Parameter Identification

**5.1 Background.** In this section, the authors provide several updates to the two model parameter identification studies that were presented in Ref. [13], and offer an additional model parameter identification study based on an impact experiment that showcases the effect of external forces on the relationship between the initial relative velocity and CoR. The goal of all studies was to identify the parameters of the BWSHCCM (or the NDBWSHCCM) and the BWMCM (or the NDBWMCM) in a manner such that the results of the numerical simulations of the models correlate well with the experimental data, showcasing that the models are suitable for the description of a variety of collision phenomena.

It is assumed that the experimental data are provided either in the form of a finite sequence of measured relative velocities of the bodies at the time of the collision  $\tilde{v}_0 \in \mathbb{R}_{>0}^M$  and a finite sequence of the corresponding measured CoRs  $\tilde{e} \in [0, 1]^M$  with  $M \in \mathbb{Z}_{\geq 1}$ , or in the form of hysteresis loops:  $M \in \mathbb{Z}_{\geq 1}$  sequences indexed by  $j \in \{1, \dots, M\} \subseteq \mathbb{Z}$  that contain the contact force data  $\tilde{F}_j \in \mathbb{R}^{K_j}$  vs. displacement data  $\tilde{x}_j \in \mathbb{R}^{K_j}$  with each  $K_j \in \mathbb{Z}_{\geq 1}$ . It is also assumed that the external force  $u_i \in \mathcal{U}_1$  is known for each individual measurement (i.e., for each  $i \in \{1, \dots, M\} \subseteq \mathbb{Z}$ ).

If the identification is performed based on the CoR data, then the quality of the base parameterization  $P^* \in \mathbb{P}^*$  of the NDBWSHCCM or the NDBWMCM may be assessed by the cost function  $J : \mathbb{R}_{>0}^M \times [0, 1]^M \times \mathbb{P}^* \rightarrow \mathbb{R}_{\geq 0}$  given by

$$J(\tilde{v}_0, \tilde{e}, P^*) \triangleq \frac{1}{M} \sum_{i=1}^M (\tilde{e}_i - e(\mathcal{P}(P^*, \tilde{v}_{0,i})))^2 \quad (32)$$

which corresponds to the mean squared modeling error. The identification of the model parameters based on the hysteresis data was performed using an ad-hoc procedure, and its detailed description will be omitted for the sake of brevity. In both cases, the quality of the parameterizations can also be assessed by inspecting the plotted data.

For the sake of reproducibility, it is remarked that the numerical simulation and the data analysis that are described in this section were performed using Python 3.11.0, NumPy 1.24.2 [36], and SciPy 1.14.0 [37], and relied on the IEEE-754 floating point arithmetic (with the default rounding mode) for the quantization of real numbers [38]. All numerical simulations were performed using the explicit Runge-Kutta method of order 8 [39–41] available via the interface of the function `integrate.solve_ivp` from the library SciPy 1.14.0 [37]. All settings of `integrate.solve_ivp` were left at their default values, with the exception of the maximum time step (`max_step`), the relative tolerance (`rtol`), and the absolute tolerance (`atol`): the relative tolerance was set to  $\approx 10^{-10}$  and the absolute tolerance was set to  $\approx 10^{-12}$ . The code is available from the personal repository of the corresponding author.<sup>11</sup>

Lastly, before proceeding with the description of the model parameter identification studies, it should be remarked that due to the nature of the methodology that was chosen for the identification of the models, any apparent discrepancies in the quality of the parameterizations obtained using different models are not indicative of the capabilities of the models, as the authors largely relied on the numerical local (constrained) optimization to refine the parameters of the models from an initial guess. The goal of the studies

**Table 2** Material properties for DSS and DSA ( $\rho$  is the density,  $E$  is the modulus of elasticity,  $\nu$  is the Poisson's ratio)

Parameter	EN9 Steel	Aluminum Alloy	Aluminum Oxide
$\rho$ (kg m <sup>-3</sup> )	7850	2700	3960
$E$ (Pa)	$205 \times 10^9$	$70 \times 10^9$	$370 \times 10^9$
$\nu$ (-)	0.29	0.33	0.22

presented below is merely to provide evidence that both models are capable of providing an adequate description of the physical phenomena described by the data.

**5.2 Kharaz and Gorham (2000).** The first parameter identification study that was presented in Ref. [13] employed the experimental datasets provided in Fig. 1 in Ref. [31]:

- “dataset steel” (DSS): CoR vs. initial relative velocity for the normal impact of a 5 mm diameter aluminum oxide sphere on a thick EN9 steel plate.
- “dataset aluminum” (DSA): CoR vs. initial relative velocity for the normal impact of a 5 mm diameter aluminum oxide sphere on a thick aluminum alloy plate.

The data were extracted using the image processing software Web-PlotDigitizer [42]. In both experiments, the plates were fixed to the ground, and the spheres were dropped from a fixed height, gaining the velocity under the influence of the force of gravity on Earth. It is interesting to note that no justification was provided for not taking into account the influence of the force of gravity in the parameter identification study that was performed in Ref. [13]. Nonetheless, this omission is conventional, as the influence of the force of gravity for impacts of a sphere on a flat is insignificant unless the ratio of the time scale to the initial relative velocity is high, that is,  $\gg 10^{-4} \text{ s}^2 \text{ m}^{-1}$  (e.g., see Ref. [27]). Up to an order of magnitude, the time scale for DSS and DSA may be approximated as

$$T_c \approx \left(\frac{m}{k}\right)^{\frac{1}{p+1}} v_0^{-\frac{p-1}{p+1}}$$

where  $m \in \mathbb{R}_{>0}$  is the mass of a sphere,  $k \in \mathbb{R}_{>0}$  is the effective stiffness (to be explained later),  $v_0 \in \mathbb{R}_{>0}$  is the initial relative velocity and  $p \in \mathbb{R}_{\geq 1}$  is a geometry-dependent parameter (to be explained later). Then,

$$\frac{T_c}{v_0} \approx \left(\frac{m}{k}\right)^{\frac{1}{p+1}} v_0^{-\frac{2p}{p+1}}$$

Since it is of interest to find the maximum value of this ratio, it suffices to consider the lower bound on the initial relative velocity such as  $v_0 = 10^{-1} \text{ m s}^{-1}$ , which can be used both for DSS and DSA (it should be noted that this bound is very conservative). The mass of each sphere can be calculated based on the assumptions about material properties and the geometry of a sphere. It is given by (e.g., see Section 6.7 in Ref. [43] and Section 2.1 in Ref. [44])

$$m \approx \frac{4}{3} \pi \rho a^3$$

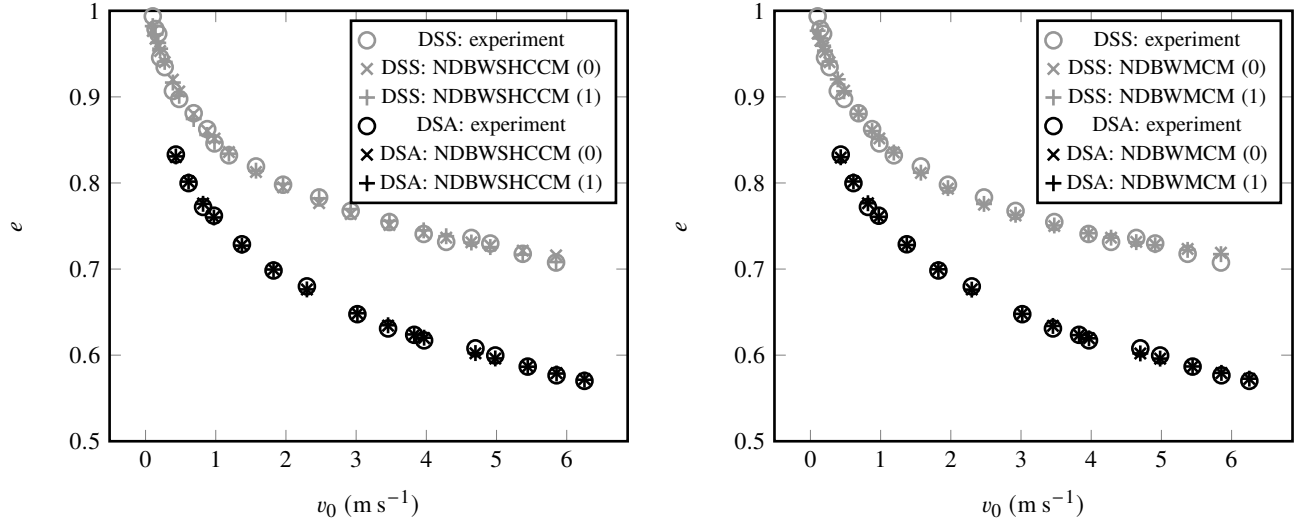
where  $\rho$  is the density of the material of the spheres (aluminum oxide) and  $a \approx 2.5 \times 10^{-3} \text{ m}$  is the radius of the spheres. The effective stiffness  $k$  and the exponent  $p$  may be estimated based on the Hertzian contact theory for a parabolic indenter ([45, 46], see also Ref. [47]). Thus,  $p \approx 3/2$  and

$$k \approx \frac{4}{3} E^* \sqrt{a}$$

<sup>11</sup><https://gitlab.com/user9716869/EBWCL>

**Table 3 DSS and DSA: parameter identification: the columns labeled DSS (0) and DSA (0) provide the data that were obtained based on the results previous study, the columns labeled DSS (1) and DSA (1) provide the data that were obtained based on the results of the present study; the value of  $U_b$  is irrelevant as it was assumed that  $u = 0$**

	NDBWSHCCM				NDBWMCM			
$P^*$ and $J$	DSS (0)	DSS (1)	DSA (0)	DSA (1)	DSS (0)	DSS (1)	DSA (0)	DSA (1)
$B_b$	1.43	2.38	0.63	1.04	0.655	0.966	0.44	0.521
$\Gamma_b$	-1.42	-2.38	-0.611	-1.02	-0.64	-0.966	-0.418	-0.521
$\kappa$	0.632	0.677	0.188	0.362	0.519	0.531	0.113	0.168
$\sigma_b$	0.00715	0.0348	0.00594	0.017	0.0118	$2.22 \times 10^{-16}$	0.00785	0.0144
$n$	1.31	2.93	1	1.01	1.94	1.57	1.27	1
$p$	1.27	2.62	2.02	1.67	2.28	1.75	3.14	2.04
$U_b$	n/a	n/a	n/a	n/a	n/a	n/a	n/a	n/a
$J(\tilde{v}_0, \tilde{e}, P^*)$	$5.81 \times 10^{-5}$	$3.51 \times 10^{-5}$	$7.62 \times 10^{-6}$	$7.23 \times 10^{-6}$	$7.49 \times 10^{-5}$	$6.05 \times 10^{-5}$	$8.07 \times 10^{-6}$	$8.02 \times 10^{-6}$



(a) CoR: NDBWSHCCM vs. experiment: NDBWSHCCM (0) represents the data from the previous study, NDBWSHCCM (1) represents the data from the present study  
(b) CoR: NDBWMCM vs. experiment: NDBWMCM (0) represents the data from the previous study, NDBWMCM (1) represents the data from the present study

**Fig. 1 Kharaz and Gorham (2000): CoR: models vs. experiment**

with  $E^*$  being the effective modulus of elasticity given by

$$E^* = \frac{E_1 E_2}{E_1 + E_2 - E_2 \nu_1^2 - E_1 \nu_2^2}$$

where  $E_1$  is the modulus of elasticity of the material of the spheres,  $E_2$  is the modulus of elasticity of the plate,  $\nu_1$  is the Poisson's ratio of the material of the spheres,  $\nu_2$  is the Poisson's ratio of the material of the plate. The material properties were acquired from Ref. [48] and listed in Table 2. The calculated values of  $T_c/v_0$  are  $\approx 5.96 \times 10^{-5} \text{ s}^2 \text{ m}^{-1}$  for DSS and  $\approx 8.12 \times 10^{-5} \text{ s}^2 \text{ m}^{-1}$  for DSA. Both values are below the threshold value. Therefore, it was acceptable to ignore the force of gravity in the model parameter identification study performed in Ref. [13]. The shape of the CoR vs.  $v_0$  curves associated with DSS and DSA also suggests that the role of the force of gravity was insignificant: usually, the force of gravity acts to reduce the CoR significantly at low  $v_0$  (see Refs. [24, 27] and Subsection 5.4). However, this reduction in CoR at low velocities is not present in DSS and DSA. The force of gravity will also be ignored in the model parameter identification study in this article.

The model parameter identification study described in Ref. [13] is repeated using an implementation of the algorithm COBYQA [49–51] available via the interface of the SciPy function `optimize.minimize`. As previously, the simulations were performed

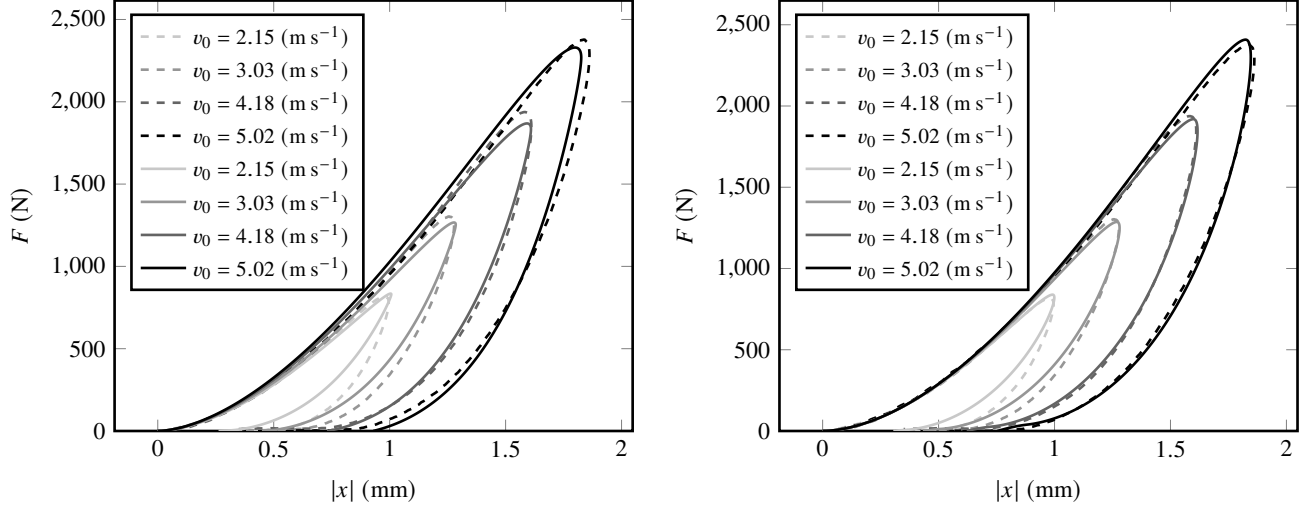
using the maximum time step of  $\approx 10^{-2}$ . The approximations of the values of the identified parameters and the associated values of the cost function are shown in Table 3. Figure 1(a) shows the plots of CoR against the initial relative velocity obtained experimentally and from the results of the numerical simulations of the NDBWSHCCM. Figure 1(b) shows the plots of CoR against the initial relative velocity obtained experimentally and from the results of the numerical simulations of the NDBWMCM. As can be seen from the values of the cost function, the authors were able to improve upon the results obtained in the previous study, albeit the improvements were marginal. Nonetheless, the authors believe that it was important to repeat the study with fewer constraints imposed on the parameters of the NDBWMCM.

**5.3 Cross (2011).** This subsection presents an update to the model parameter identification study based on the experimentally obtained hysteresis data that was performed in Ref. [13]. The experimentally obtained hysteresis data were provided by Professor Rodney Cross and appeared in Fig. 9.5 in Ref. [32].

The methodology that was employed for all simulations that were used to develop the results that are presented in this subsection was explained in Subsection 5.1; the maximum time step for the simulations upon which the data presented in this subsection are based was set to  $\approx T_c/100 \text{ s}$ . For the purposes of the identification of the parameters of the NDBWSHCCM and the NDBWMCM,

**Table 4** Normal impact of a baseball on a flat surface: parameterization of the BWSHCCM and the BWMCM

Parameter	BWSHCCM	BWMCM
$m$	0.145 (kg)	0.145 (kg)
$k$	117080063 (kg m <sup>1-p</sup> s <sup>-2</sup> )	253000000 (kg m <sup>1-p</sup> s <sup>-2</sup> )
$c$	5854003 (kg m <sup>-p</sup> s <sup>-1</sup> )	2811 (kg s <sup>-1</sup> )
$n$	1.1 (-)	1.2 (-)
$p$	1.7 (-)	1.8 (-)
$\alpha$	0.1 (-)	0.15 (-)
$\beta$	981.05 (m <sup>-n</sup> )	1200 (m <sup>-n</sup> )
$\gamma$	-961.4 (m <sup>-n</sup> )	-1200 (m <sup>-n</sup> )
$A$	0.925 (-)	1.01 (-)



(a) Normal impact of a baseball on a flat surface: experimentally obtained hysteresis loops (dashed lines) vs. hysteresis loops obtained from the numerical simulations of the BWSHCCM (solid lines)

(b) Normal impact of a baseball on a flat surface: experimentally obtained hysteresis loops (dashed lines) vs. hysteresis loops obtained from the numerical simulations of the BWMCM (solid lines)

**Fig. 2** CoR: models vs. experiment

it was assumed that the only known model parameter was the mass of the ball: its value (0.145 kg) was reported in Ref. [32]. Furthermore, due to the nature of the experiment, it was deemed appropriate to ignore the effect of external forces ( $u = 0$  N).

Figure 2 shows the plots of the experimentally obtained hysteresis loops observed during the normal impact of a baseball on a flat surface across a range of initial relative velocities, and the hysteresis loops obtained based on the results of the numerical simulations of the BWSHCCM and the BWMCM with the parameters shown in Table 4. The plots demonstrate a good agreement between the experimentally obtained hysteresis loops and the hysteresis loops obtained from the simulation of the BWSHCCM and the BWMCM. As mentioned in Section 1, in the previous study [13], only the parameters of the NDBWSHCCM were identified. Therefore, the study presented in this subsection shows that BWMCM can also adequately represent the collision phenomenon that was described in Ref. [32].

**5.4 Quinn (2004).** The final parameter identification study will employ the experimental dataset provided in Fig. 3 a in Ref. [24]. The figure visualizes the CoR vs. initial relative velocity data obtained from the measurements of the repeated normal impacts of a pin-jointed rod with a hemispherical indenter attached to its end on a flat surface under the influence of the force of gravity. The data were obtained in conditions such that the force of gravity has a non-negligible effect on the relationship between CoR and the initial relative velocity (see Ref. [24] and the discussion in Subsection 5.2). The data were extracted using the image processing software WebPlotDigitizer [42].

It should be noted that the applicability of the NDBMSHCCM and the NDBWMCM to the description of the experiment in Ref. [24] may be questioned due to the presence of a pin joint constraint and a rod whose inertial properties are non-negligible in comparison to the indenter. Nonetheless, since the typical CoR vs. initial relative velocity curves for unconstrained systems are expected to follow a similar profile, it was deemed that the experimental data were adequate for the model validation. It was assumed that the external force is constant  $u \triangleq -mg$ , where  $m$  is the effective mass of the system and  $g \triangleq 9.80665$  m s<sup>-2</sup> is the gravitational acceleration (e.g., see Ref. [52]). No assumption was made about the value of the effective mass  $m$  of the system. Therefore, only the value of  $U_b m$  is identified and reported upon.

The methodology that was used for the model parameter identification was identical to the one employed in Subsection 5.2. The experimental data and the results of the identification are shown in Figure 3. The identified parameters are shown in Table 5. In this case, it was not possible to achieve a nearly perfect match between the experimental data and the results of the simulation (cf. Subsection 5.2) using either collision model. Nonetheless, qualitatively, the simulation data exhibit the primary feature of interest in the experimental data: rapid decline of CoR as the initial relative velocity decreases.

## 6 Conclusions and Future Work

The article provided extensions of two mathematical models of binary direct collinear collisions of convex viscoplastic bodies (BWSHCCM and BWMCM) that take into account the effects of

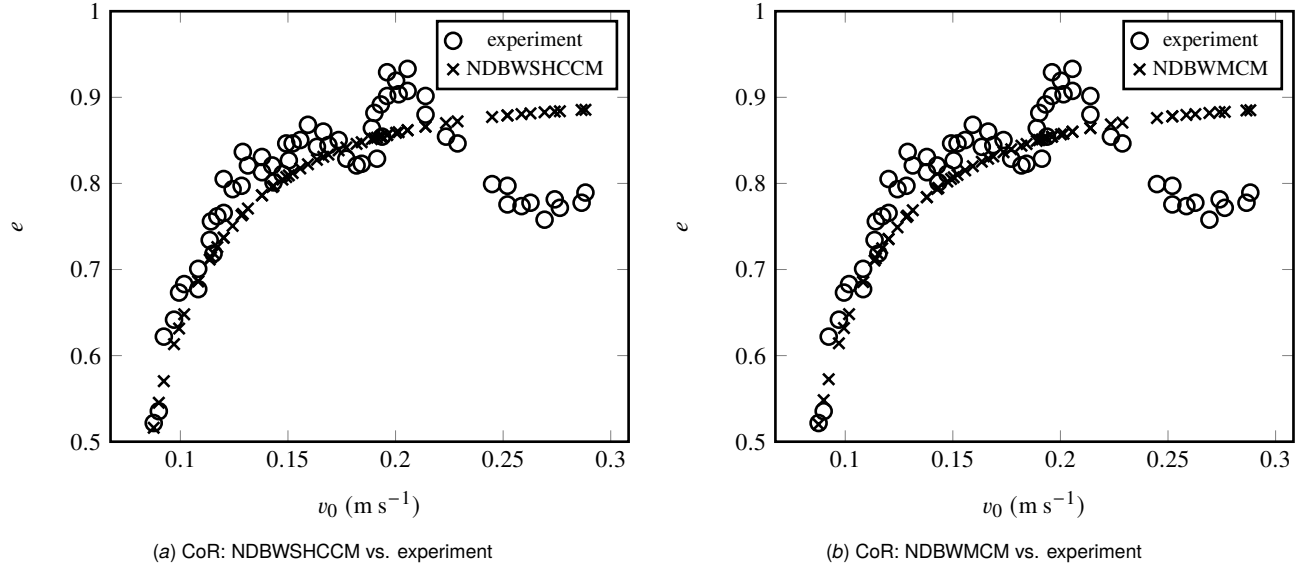


**Fig. 3** Quinn (2004): CoR: models vs. experiment

**Table 5** Quinn (2004): parameter identification (the dimensional parameters are stated in the SI base units)

$P^*$ and $J$	NDBWSHCCM	NDBWMCM
$B_b$	1.05	0.529
$\Gamma_b$	-1.05	-0.273
$\kappa$	0.77	0.518
$\sigma_b$	0.0638	0.0155
$n$	1.96	1.86
$p$	1	1.01
$U_b m$	0.02	0.0181
$J(\tilde{v}_0, \tilde{e}, P^*)$	0.00294	0.00303

external forces that may act on the bodies during the collision process. Furthermore, the article proposes an alternative form of the BWMCM, and the analysis of the BWMCM was extended to consider certain corner cases that were not considered previously in the research literature, to the best knowledge of the authors.

From the perspective of the future work, in Ref. [13], the authors have already identified several possible directions for further development of the modeling framework associated with the BWSHCCM and the BWMCM. As of the work presented in this article, it will be useful to extend the modeling framework to other function spaces for the input signals (e.g., continuous bounded functions). Finally, it may also be useful to extend the binary collision model presented in this article to binary collisions of multi-body systems or simultaneous collisions of multiple bodies (e.g., see Refs. [5, 33]). It may also be interesting to consider applications of the models that involve external forces other than the force of gravity. Lastly, it may be beneficial to consider collision laws developed based on the hysteresis models other than the Bouc-Wen models (e.g., some of the hysteresis models that appeared recently in the research literature include [53–58]).

## Acknowledgment

The authors would like to acknowledge their families, colleagues, and friends. Special thanks go to Professor Rodney Cross for providing experimental data from Ref. [32]. Special thanks also go to the members of Staff of Auburn University Libraries for their assistance in finding rare and out-of-print research articles and research monographs. The authors would also like to acknowledge the professional online communities, instructional websites, and various online ser-

vice providers, especially <https://www.adobe.com/acrobat/online/pdf-to-word.html>, <https://automeris.io>, <https://capitalizemytitle.com>, <https://www.matweb.com>, <https://www.overleaf.com>, <https://pgfplots.net>, <https://scholar.google.com>, <https://stackexchange.com>, <https://stringtranslate.com>, <https://www.wikipedia.org>. We also note that the results of some of the calculations that are presented in this article were performed with the assistance of the software Wolfram Mathematica [59]. Other software that was used to produce this article included Adobe Acrobat Reader, Adobe Digital Editions, DiffMerge, Git, GitLab, Google Chrome, Google Gemini, Grammarly (the use of Grammarly was restricted to the identification and correction of spelling, grammar, and punctuation errors), Jupyter Notebook, LibreOffice, macOS Monterey, Mamba, Microsoft Outlook, Preview, Safari, TeX Live/MacTeX, Texmaker, and Zotero.

## Funding Data

The present work did not receive any specific funding. However, the researchers receive financial support from Auburn University for their overall research activity.

## Appendix A: Notation and Conventions

The notation is adopted from Ref. [13], and will not be restated fully. Essentially all of the definitions and results that are employed in this article are standard in the fields of set theory, general topology, analysis, ordinary differential equations, and nonlinear systems/control. They can be found in a number of textbooks and monographs on these subjects (e.g., see Refs. [43, 60–68]).



Nonetheless, the article employs several concepts that have not appeared in Ref. [13]. The majority of these concepts are related to the description of dynamics of time-variant systems.

**Definition A.1.** Consider the following system of ordinary differential equations

$$\dot{x} = f(t, x) \quad (\text{A1})$$

where  $f : \mathbb{R}_{\geq 0} \times \mathbb{R}^n \rightarrow \mathbb{R}^n$  with  $n \in \mathbb{Z}_{\geq 1}$  is the state function that is continuous in the first argument ( $t$ ) and locally Lipschitz continuous in the second argument ( $x$ ). Equation (A1) augmented with an initial condition  $x(t_0) = x_0 \in \mathbb{R}^n$  where  $t_0 \in \mathbb{R}_{\geq 0}$  shall be referred to as an initial value problem (IVP) associated with the system given by Eq. (A1). A differentiable function  $x : J \rightarrow \mathbb{R}^n$  with  $J \triangleq [t_0, t_0 + T)$  and  $T \in \mathbb{R}_{>0} \cup \{+\infty\}$  is a solution of the IVP associated with the system given by Eq. (A1) with the initial condition  $x_0 \in \mathbb{R}^n$  if  $x(t_0) = x_0$  and  $\dot{x}(t) = f(t, x(t))$  for all  $t \in J$ . The system given by Eq. (A1) may also have an output, which is expressed by the relation  $y = g(x)$ , where  $g : \mathbb{R}^n \rightarrow \mathbb{R}^m$  with  $m \in \mathbb{Z}_{\geq 1}$  is a continuous function.

The following definitions were adopted from Ref. [65].<sup>12</sup>

**Definition A.2.** The solutions of the system given by Eq. (A1) are said to be uniformly bounded if and only if for all  $\alpha \in \mathbb{R}_{>0}$ , there exists  $\beta \in \mathbb{R}_{>0}$  such that  $\|x(t)\| < \beta$  for all  $t \in [t_0, t_0 + T)$  for every solution  $x : [t_0, t_0 + T) \rightarrow \mathbb{R}^n$  with  $t_0 \in \mathbb{R}_{\geq 0}$  and  $T \in \mathbb{R}_{>0} \cup \{+\infty\}$  starting from the initial condition  $x(t_0) = x_0 \in \mathbb{R}^n$  such that  $\|x_0\| \leq \alpha$ .

## Appendix B: Analysis of the BWSHCCM

Here, the NDBWSHCCM is considered under the assumption that the initial conditions are arbitrary and the values of the parameters are restricted to  $B \in \mathbb{R}_{\geq 0}$ ,  $\Gamma \in [-B, B]$ ,  $\kappa \in (0, 1)$ ,  $\sigma \in \mathbb{R}_{\geq 0}$ ,  $n, p \in \mathbb{R}_{\geq 1}$  (as previously,  $\kappa_c = 1 - \kappa$ ).

Define  $\mathcal{W} : \mathbb{R}^3 \rightarrow \mathbb{R}$  as

$$\mathcal{W}(\mathbf{X}) \triangleq \frac{\kappa}{p+1} |X|^{p+1} + \frac{\kappa_c}{p+1} |Z|^{p+1} + \frac{1}{2} V^2$$

for all  $\mathbf{X} \triangleq (X, Z, V) \in \mathbb{R}^3$ . Define  $E : \mathbb{R}_{\geq 0} \rightarrow \mathbb{R}$  as

$$E(T) \triangleq \int_0^T |U(s)| ds$$

and denote

$$E(+\infty) \triangleq \lim_{T \rightarrow +\infty} \int_0^T |U(s)| ds$$

It should be noted that  $E(+\infty) \in \mathbb{R}_{\geq 0}$ . Define the Lyapunov candidate  $\mathcal{V} : \mathbb{R}_{\geq 0} \times \mathbb{R}^3 \rightarrow \mathbb{R}$  as<sup>13</sup>

$$\mathcal{V}(T, \mathbf{X}) \triangleq e^{-E(T)} \mathcal{W}(\mathbf{X})$$

Define  $\mathcal{W}' : \mathbb{R}^3 \rightarrow \mathbb{R}$  as

$$\mathcal{W}'(\mathbf{X}) \triangleq -\sigma |X|^{pV^2} - \kappa_c |Z|^{p+n-1} (B|Z||V| + \Gamma ZV)$$

for all  $\mathbf{X} \in \mathbb{R}^3$ . Referring to Ref. [13], note that

$$\dot{\mathcal{W}}(T, \mathbf{X}) = \mathcal{W}'(\mathbf{X}) + U(T)V$$

for all  $T \in \mathbb{R}_{\geq 0}$  and  $\mathbf{X} \in \mathbb{R}^3$ . Thus,

$$\dot{\mathcal{V}}(T, \mathbf{X}) = e^{-E(T)} (U(T)V - |U(T)|\mathcal{W}(\mathbf{X})) + e^{-E(T)} \mathcal{W}'(\mathbf{X})$$

for all  $T \in \mathbb{R}_{\geq 0}$  and  $\mathbf{X} \in \mathbb{R}^3$ . Define  $K \in \mathbb{R}_{\geq 0}$  as

$$K \triangleq \max \left( \frac{p+1}{\kappa}, \frac{p+1}{\kappa_c} \right)$$

<sup>12</sup> $\|\cdot\|$  denotes an arbitrary norm on  $\mathbb{R}^n$ .

<sup>13</sup>This form of the Lyapunov function was inspired by Example 10.1 in Ref. [65].

**Lemma B.1.** Under the restrictions on the values of the parameters stated above,  $\dot{\mathcal{V}}(T, \mathbf{X}) \leq 0$  for all  $T \in \mathbb{R}_{\geq 0}$  and  $\mathbf{X} \in \mathbb{R}^3$  such that  $K \leq \|\mathbf{X}\|_{\infty}$ .<sup>14</sup>

*Proof.* Note that  $\mathcal{W}'(\mathbf{X}) \leq 0$  for all  $\mathbf{X} \in \mathbb{R}^3$  (a proof can be found in Ref. [13]). Also,  $2 \leq K$  because  $(p+1)/\kappa \leq K$ ,  $\kappa \in (0, 1)$ , and  $1 \leq p$ .

Fix  $T \in \mathbb{R}_{\geq 0}$  and  $\mathbf{X} \in \mathbb{R}^3$  such that  $K \leq \|\mathbf{X}\|_{\infty}$ . Since  $\mathcal{W}'(\mathbf{X}) \leq 0$ , to show that  $\dot{\mathcal{V}}(T, \mathbf{X}) \leq 0$ , it suffices to show that  $U(T)V \leq |U(T)|\mathcal{W}(\mathbf{X})$ . Thus, it suffices to show that  $|V| \leq \mathcal{W}(\mathbf{X})$ . There are three cases to consider

- Case I:  $\|\mathbf{X}\|_{\infty} = |X|$ . It then follows that  $(p+1)/\kappa \leq K \leq |X|$  or  $1 \leq \kappa/(p+1)|X|$ ,  $1 \leq |X|$  and  $|V| \leq |X|$ . Therefore,

$$|V| \leq |X| \leq |X|^p \leq \frac{\kappa}{p+1} |X|^{p+1} \leq \mathcal{W}(\mathbf{X})$$

- Case II:  $\|\mathbf{X}\|_{\infty} = |Z|$ . The proof of  $|V| \leq \mathcal{W}(\mathbf{X})$  follows from Case I mutatis mutandis.
- Case III:  $\|\mathbf{X}\|_{\infty} = |V|$ . Then,  $2 \leq K \leq |V|$ . Thus,

$$|V| \leq \frac{1}{2} V^2 \leq \mathcal{W}(\mathbf{X})$$

Thus,  $\dot{\mathcal{V}}(T, \mathbf{X}) \leq 0$ . By generalization, this holds for all  $T \in \mathbb{R}_{\geq 0}$  and  $\mathbf{X} \in \mathbb{R}^3$  such that  $K \leq \|\mathbf{X}\|_{\infty}$ .  $\square$

**Proposition B.2.** Under the restrictions on the values of the parameters stated above, there exists a unique solution of the NDBWSHCCM on any time interval  $[T_0, T_0 + T)$  with  $T_0 \in \mathbb{R}_{\geq 0}$  and  $T \in \mathbb{R}_{>0} \cup \{+\infty\}$  for every initial condition  $(X_0, Z_0, V_0) \in \mathbb{R}^3$ . Furthermore, the solutions of the NDBWSHCCM are uniformly bounded.

*Proof.* Taking into account that the state function of the NDBWSHCCM is locally Lipschitz continuous in  $\mathbf{X}$  and continuous in  $T$ , the solutions of the NDBWSHCCM exist and are unique on a non-empty maximal interval of existence (e.g., see Theorem 54 in Ref. [66] or Theorem 2.38 in Ref. [67]). Noting that  $\mathcal{W}$  and  $\mathcal{V}$  are continuously differentiable,  $\mathcal{W}$  is radially unbounded,

$$e^{-E(+\infty)} \mathcal{W}(\mathbf{X}) \leq \mathcal{V}(T, \mathbf{X}) \leq \mathcal{W}(\mathbf{X})$$

for all  $T \in \mathbb{R}_{\geq 0}$  and  $\mathbf{X} \in \mathbb{R}^3$ , and  $\dot{\mathcal{V}}(T, \mathbf{X}) \leq 0$  for all  $T \in \mathbb{R}_{\geq 0}$  and  $\mathbf{X} \in \mathbb{R}^3$  such that  $K \leq \|\mathbf{X}\|_{\infty}$  (by Lemma B.1), the solutions of the NDBWSHCCM are uniformly bounded by Theorem 8.8 in Ref. [65]. Therefore, by the theorem on the extendability of the solutions (e.g., see Proposition C.3.6 in Ref. [66] or Theorem 2.39 in Ref. [67]), each solution can be extended to a unique solution on  $[T_0, +\infty)$ .  $\square$

## Appendix C: Analysis of the BWCM

Firstly, we note that the solutions of the model given by Eq. (25) and Eq. (26) are identical to the solutions of the model given by Eq. (4) and Eq. (6) under the assumption that  $u = 0$ . Suppose that the outputs of both models are  $(r, y, z, w, x, v)$ . Given  $v_0 \in \mathbb{R}_{>0}$ , suppose that  $(r, y, z, w, x, v)$  is the output of the model given by Eq. (4) and Eq. (6). Noting that  $\dot{w} = -\dot{r} + \dot{v}$  and integrating it on both sides results in  $w - w(0) = \dot{r} - \dot{r}(0) + v - v(0)$ . This is equivalent to  $w = \dot{r} + v$ . Expanding  $\dot{r}$  and taking into account that  $\dot{y} = w$  yields

$$\dot{y} = w = -\alpha \frac{k}{c} |y|^{p-1} y - \alpha_c \frac{k}{c} |z|^{p-1} z + v$$

which implies that  $w$ ,  $y$ ,  $z$  and  $v$  satisfy the relation given by Eq. (26) and the second relation associated with Eq. (25).

<sup>14</sup>Note that  $\|\mathbf{x}\|_{\infty} \triangleq \max(|x_1|, \dots, |x_n|)$  denotes the standard  $\infty$ -norm on  $\mathbb{R}^n$ .

Other relations associated with the state function of the model given by Eq. (25) are satisfied trivially. Therefore, every solution of the model given by Eq. (4) and Eq. (6) is also a solution of the model given by Eq. (25) and Eq. (26). It is also sufficiently simple to check that every solution of the model given by Eq. (25) and Eq. (26) is a solution of the model given by Eq. (4) and Eq. (6).

Since the state function of the model given by Eq. (25) is locally Lipschitz, its solutions are unique (so long as they exist). Suppose that the model given by Eq. (4) and Eq. (6) has two distinct solutions starting from the same initial condition. Then, the model given by Eq. (25) and Eq. (26) has two distinct solutions starting from the same initial condition, which results in a contradiction. Therefore, the solutions of the model given by Eq. (25) and Eq. (26) are unique.

Further analysis will be performed on the NDBWMCM (given by Eq. (28)). Firstly, it is remarked that the state  $X$  can be recovered by noticing that  $X = R + Y$ . Thus, for the purposes of the analysis presented in this section, the model given by Eq. (28) is reduced to

$$\begin{cases} \dot{R} = \kappa\sigma|Y|^{p-1}Y + \kappa_c\sigma|Z|^{p-1}Z \\ \dot{Y} = -\kappa\sigma|Y|^{p-1}Y - \kappa_c\sigma|Z|^{p-1}Z + V \\ \dot{Z} = \dot{Y} - B|Z|^{n-1}Z|\dot{Y}| - \Gamma|Z|^n\dot{Y} \\ \dot{V} = -\kappa|Y|^{p-1}Y - \kappa_c|Z|^{p-1}Z + U \end{cases} \quad (C1)$$

It shall also be assumed that the initial conditions are arbitrary real numbers and the values of the parameters are restricted to  $B \in \mathbb{R}_{\geq 0}$ ,  $\Gamma \in [-B, B]$ ,  $\kappa \in (0, 1)$ ,  $\sigma \in \mathbb{R}_{> 0}$ ,  $n, p \in \mathbb{R}_{\geq 1}$  (as previously,  $\kappa_c = 1 - \kappa$ ).

Define  $\mathcal{W} : \mathbb{R}^4 \rightarrow \mathbb{R}$  as

$$\mathcal{W}(\mathbf{X}) \triangleq (R + \sigma V)^2 + \frac{\kappa}{p+1}|Y|^{p+1} + \frac{\kappa_c}{p+1}|Z|^{p+1} + \frac{1}{2}V^2$$

for all  $\mathbf{X} \triangleq (R, Y, Z, V) \in \mathbb{R}^4$ . Define also  $E : \mathbb{R}_{\geq 0} \rightarrow \mathbb{R}$  as

$$E(T) \triangleq \int_0^T |U(s)|ds$$

and denote

$$E(+\infty) \triangleq \lim_{T \rightarrow +\infty} \int_0^T |U(s)|ds$$

It should be noted that  $E(+\infty) \in \mathbb{R}_{\geq 0}$ . Define the Lyapunov candidate  $\mathcal{V} : \mathbb{R}_{\geq 0} \times \mathbb{R}^4 \rightarrow \mathbb{R}$  as<sup>15</sup>

$$\mathcal{V}(T, \mathbf{X}) \triangleq e^{-E(T)}\mathcal{W}(\mathbf{X})$$

Define  $\mathcal{W}' : \mathbb{R}^4 \rightarrow \mathbb{R}$  as

$$\mathcal{W}'(\mathbf{X}) \triangleq -\frac{1}{\sigma}\dot{R}^2 - \kappa_c|Z|^{p+n-1}(B|Z||V - \dot{R}| + \Gamma Z(V - \dot{R}))$$

and  $\mathcal{W}'' : \mathbb{R}^4 \rightarrow \mathbb{R}$  as

$$\mathcal{W}''(\mathbf{X}) \triangleq (2\sigma^2 + 1)V + 2\sigma R$$

for all  $\mathbf{X} \in \mathbb{R}^4$  (it should be remarked that  $\dot{R}$  is used as an abbreviation for  $\kappa\sigma|Y|^{p-1}Y + \kappa_c\sigma|Z|^{p-1}Z$ ). Referring to Ref. [13], note that

$$\dot{\mathcal{V}}(T, \mathbf{X}) = \mathcal{W}'(\mathbf{X}) + U(T)\mathcal{W}''(\mathbf{X})$$

for all  $T \in \mathbb{R}_{\geq 0}$  and  $\mathbf{X} \in \mathbb{R}^4$ . Thus,

$$\dot{\mathcal{V}}(T, \mathbf{X}) = e^{-E(T)}(U(T)\mathcal{W}''(\mathbf{X}) - |\mathcal{W}'(\mathbf{X})| + e^{-E(T)}\mathcal{W}'(\mathbf{X}))$$

for all  $T \in \mathbb{R}_{\geq 0}$  and  $\mathbf{X} \in \mathbb{R}^4$ . Define  $K \in \mathbb{R}_{\geq 0}$  as

$$K \triangleq (2\sigma^2 + 2\sigma + 1) \max\left(2\sigma^2 + 1, \frac{p+1}{\kappa}, \frac{p+1}{\kappa_c}\right)$$

<sup>15</sup>This form of the Lyapunov function was inspired by Example 10.1 in Ref. [65].

**Lemma C.1.** Under the restrictions on the values of the parameters stated above,  $\dot{\mathcal{V}}(T, \mathbf{X}) \leq 0$  for all  $T \in \mathbb{R}_{\geq 0}$  and  $\mathbf{X} \in \mathbb{R}^4$  such that  $K \leq \|\mathbf{X}\|_{\infty}$ .

*Proof.* Note that  $\mathcal{W}'(\mathbf{X}) \leq 0$  for all  $\mathbf{X} \in \mathbb{R}^4$  (see Lemma C.1 in Ref. [13] for a proof; it should be remarked that Lemma C.1 in Ref. [13] holds also under the less restrictive ranges of the parameters that are used in this study). Fix  $T \in \mathbb{R}_{\geq 0}$  and  $\mathbf{X} \in \mathbb{R}^4$  such that  $K \leq \|\mathbf{X}\|_{\infty}$ . Since  $\mathcal{W}'(\mathbf{X}) \leq 0$ , it suffices to show that

$$U(T)((2\sigma^2 + 1)V + 2\sigma R) \leq |U(T)|\mathcal{W}(\mathbf{X})$$

Therefore, it suffices to show that

$$|(2\sigma^2 + 1)V + 2\sigma R| \leq \mathcal{W}(\mathbf{X})$$

or

$$(2\sigma^2 + 1)|V| + 2\sigma|R| \leq \mathcal{W}(\mathbf{X})$$

There are four cases to consider

- Case I:  $\|\mathbf{X}\|_{\infty} = |R|$ . Then,  $|V| \leq |R|$  and

$$(2\sigma^2 + 2\sigma + 1)(2\sigma^2 + 1) \leq K \leq |R|$$

or

$$|R| \leq (2\sigma^2 + 2\sigma + 1)^{-1}(2\sigma^2 + 1)^{-1}R^2$$

Therefore,

$$\begin{aligned} (2\sigma^2 + 1)|V| + 2\sigma|R| &\leq (2\sigma^2 + 2\sigma + 1)|R| \leq \frac{1}{2\sigma^2 + 1}R^2 \\ &\leq (R + \sigma V)^2 + \frac{1}{2}V^2 \leq \mathcal{W}(\mathbf{X}) \end{aligned}$$

- Case II:  $\|\mathbf{X}\|_{\infty} = |Y|$ . Then,  $|R| \leq |Y|$ ,  $|V| \leq |Y|$ , and  $1 \leq |Y|$ . Furthermore,

$$(2\sigma^2 + 2\sigma + 1)\frac{p+1}{\kappa} \leq K \leq |Y|$$

or

$$|Y| \leq (2\sigma^2 + 2\sigma + 1)^{-1}\frac{\kappa}{p+1}Y^2$$

Therefore,

$$\begin{aligned} (2\sigma^2 + 1)|V| + 2\sigma|R| &\leq (2\sigma^2 + 2\sigma + 1)|Y| \leq \frac{\kappa}{p+1}Y^2 \\ &\leq \frac{\kappa}{p+1}|Y|^{p+1} \leq \mathcal{W}(\mathbf{X}) \end{aligned}$$

- Case III:  $\|\mathbf{X}\|_{\infty} = |Z|$ . The proof of  $|V| \leq \mathcal{W}(\mathbf{X})$  follows from Case II mutatis mutandis.
- Case IV:  $\|\mathbf{X}\|_{\infty} = |V|$ . Then,  $|R| \leq |V|$  and  $1 \leq |V|$ . Furthermore,

$$2(2\sigma^2 + 2\sigma + 1) \leq K \leq |V|$$

or

$$|V| \leq \frac{1}{2}(2\sigma^2 + 2\sigma + 1)^{-1}V^2$$

Therefore,

$$(2\sigma^2 + 1)|V| + 2\sigma|R| \leq (2\sigma^2 + 2\sigma + 1)|V| \leq \frac{1}{2}V^2 \leq \mathcal{W}(\mathbf{X})$$

Thus,  $\dot{\mathcal{V}}(T, \mathbf{X}) \leq 0$ . By generalization, this holds for all  $T \in \mathbb{R}_{\geq 0}$  and  $\mathbf{X} \in \mathbb{R}^4$  such that  $K \leq \|\mathbf{X}\|_{\infty}$ .  $\square$

**Proposition C.2.** *Under the restrictions on the values of the parameters stated above, there exists a unique solution of the NDBWMCM on any time interval  $[T_0, T_0 + T)$  with  $T_0 \in \mathbb{R}_{\geq 0}$  and  $T \in \mathbb{R}_{> 0} \cup \{+\infty\}$  for every initial condition  $(R_0, Y_0, Z_0, V_0) \in \mathbb{R}^4$ . Furthermore, the solutions of the NDBWMCM are uniformly bounded.*

*Proof.* The proof is similar to the proof of Proposition B.2.  $\square$

## References

- [1] Panagiotopoulos, P. D., 1985, *Inequality Problems in Mechanics and Applications: Convex and Nonconvex Energy Functions*, Birkhäuser, Boston, MA.
- [2] Pfeiffer, F. and Glocker, C., 2004, *Multibody Dynamics with Unilateral Contacts*, Wiley Series in Nonlinear Science, WILEY-VCH Verlag GmbH & Co. KGaA, Weinheim, The Federal Republic of Germany.
- [3] Stewart, D. E., 2011, *Dynamics with Inequalities: Impacts and Hard Constraints*, SIAM, Philadelphia, PA.
- [4] Goebel, R., Sanfelice, R. G., and Teel, A. R., 2012, *Hybrid Dynamical Systems: Modeling, Stability, and Robustness*, Princeton University Press, Princeton, NJ.
- [5] Brogliato, B., 2016, *Nonsmooth Mechanics: Models, Dynamics and Control*, 3rd ed., Communications and Control Engineering, Springer International Publishing, Cham, The Swiss Confederation.
- [6] Sanfelice, R. G., 2021, *Hybrid Feedback Control*, Princeton University Press, Princeton, NJ.
- [7] Terzopoulos, D., Platt, J., Barr, A., and Fleischer, K., 1987, "Elastically Deformable Models," *Proceedings of the 14th Annual Conference on Computer Graphics and Interactive Techniques*, Association for Computing Machinery, New York, NY, pp. 205–214, doi: [10.1145/37401.37427](https://doi.org/10.1145/37401.37427).
- [8] Platt, J. C. and Barr, A. H., 1988, "Constraint Methods for Flexible Models," *SIGGRAPH '88: Proceedings of the 15th Annual Conference on Computer Graphics and Interactive Techniques*, M. C. Stone, ed., Association for Computing Machinery, New York, NY, pp. 279–288, doi: [10.1145/54852.378524](https://doi.org/10.1145/54852.378524).
- [9] Moore, M. and Wilhelms, J., 1988, "Collision Detection and Response for Computer Animation," *SIGGRAPH '88: Proceedings of the 15th Annual Conference on Computer Graphics and Interactive Techniques*, Association for Computing Machinery, New York, NY, pp. 289–298, doi: [10.1145/54852.378528](https://doi.org/10.1145/54852.378528).
- [10] Movahedi-Lankarani, H., 1988, "Canonical Equations of Motion and Estimation of Parameters in the Analysis of Impact Problems," Ph.D., The University of Arizona, Tucson, AZ.
- [11] Machado, M., Moreira, P., Flores, P., and Lankarani, H. M., 2012, "Compliant Contact Force Models in Multibody Dynamics: Evolution of the Hertz Contact Theory," *Mechanism and Machine Theory*, **53**, pp. 99–121.
- [12] Corral, E., Moreno, R. G., García, M. J. G., and Castejón, C., 2021, "Nonlinear Phenomena of Contact in Multibody Systems Dynamics: A Review," *Nonlinear Dynamics*, **104**(2), pp. 1269–1295.
- [13] Milehins, M. and Marghitu, D. B., 2025, "The Bouc–Wen Model for Binary Direct Collinear Collisions of Convex Viscoplastic Bodies," *ASME Journal of Computational and Nonlinear Dynamics*, **20**(6), p. 061005.
- [14] Bouc, R., 1967, "Forced Vibration of Mechanical Systems with Hysteresis," *Proceedings of the Fourth Conference on Nonlinear Oscillations*, J. Gonda and F. Jelínek, eds., Academia Publishing House of the Czechoslovak Academy of Sciences, Prague, Czechoslovakia, p. 315.
- [15] Bouc, R., 1971, "Modèle mathématique d'hystérésis," *Acustica*, **24**(1), pp. 16–25.
- [16] Wen, Y.-K., 1976, "Method for Random Vibration of Hysteretic Systems," *Journal of the Engineering Mechanics Division*, **102**(2), pp. 249–263.
- [17] Ikhrouane, F. and Rodellar, J., 2007, *Systems with Hysteresis: Analysis, Identification and Control using the Bouc–Wen Model*, John Wiley & Sons, Chichester, The United Kingdom of Great Britain and Northern Ireland.
- [18] Hunt, K. H. and Crossley, F. R. E., 1975, "Coefficient of Restitution Interpreted as Damping in Vibroimpact," *ASME J Appl Mech*, **42**(2), pp. 440–445.
- [19] Maxwell, J. C., 1867, "On the Dynamical Theory of Gases," *Philosophical Transactions of the Royal Society of London*, **157**, pp. 49–88.
- [20] Johnson, K. L., 1985, *Contact Mechanics*, Cambridge University Press, Cambridge, The United Kingdom of Great Britain and Northern Ireland.
- [21] Butcher, E. A. and Segalman, D. J., 2000, "Characterizing Damping and Restitution in Compliant Impacts via Modified K-V and Higher-Order Linear Viscoelastic Models," *ASME J Appl Mech*, **67**(4), pp. 831–834.
- [22] Tatara, Y., 1977, "Effects of External Force on Contacting Times and Coefficients of Restitution in a Periodic Collision," *ASME J Appl Mech*, **44**(4), pp. 773–774.
- [23] Falcon, E., Laroche, C., Fauve, S., and Coste, C., 1998, "Behavior of One Inelastic Ball Bouncing Repeatedly off the Ground," *The European Physical Journal B - Condensed Matter and Complex Systems*, **3**(1), pp. 45–57.
- [24] Quinn, D. D., 2004, "Finite Duration Impacts With External Forces," *ASME J Appl Mech*, **72**(5), pp. 778–784.
- [25] Shen, Y., Xiang, D., Wang, X., Jiang, L., and Wei, Y., 2018, "A Contact Force Model Considering Constant External Forces for Impact Analysis in Multibody Dynamics," *Multibody System Dynamics*, **44**(4), pp. 397–419.
- [26] Xiang, D., Shen, Y., Wei, Y., and You, M., 2018, "A Comparative Study of the Dissipative Contact Force Models for Collision Under External Spring Forces," *ASME Journal of Computational and Nonlinear Dynamics*, **13**(10).
- [27] Carvalho, A. S. and Martins, J. M., 2019, "Exact Restitution and Generalizations for the Hunt–Crossley Contact Model," *Mechanism and Machine Theory*, **139**, pp. 174–194.
- [28] Chatterjee, A., James, G., and Brogliato, B., 2022, "Approximate Coefficient of Restitution for Nonlinear Viscoelastic Contact With External Load," *Granular Matter*, **24**(4), p. 124.
- [29] Akhan, A. F. and Marghitu, D. B., 2024, "Low Speed Impact of an Elastic Ball with Tapes and Clay Court," *Applied Sciences*, **14**(13), p. 5674.
- [30] Shen, Y. and Xiang, D., 2024, "A Contact Force Calculation Approach for Collision Analysis With Zero or Non-zero Initial Relative Velocity," *Nonlinear Dynamics*, **112**(22), pp. 19795–19808.
- [31] Kharaz, A. and Gorham, D., 2000, "A Study of the Restitution Coefficient in Elastic-Plastic Impact," *Philosophical Magazine Letters*, **80**(8), pp. 549–559.
- [32] Cross, R., 2011, *Physics of Baseball & Softball*, Springer Science+Business Media, New York, NY.
- [33] Stronge, W. J., 2018, *Impact Mechanics*, 2nd ed., Cambridge University Press, Cambridge, The United Kingdom of Great Britain and Northern Ireland.
- [34] Newton, I., 1729, *The Mathematical Principles of Natural Philosophy*, Printed for Benjamin Motte, at the Middle-Temple-Gate, in Fleet Street, London, Kingdom of Great Britain, Translated by Andrew Motte.
- [35] Logan, J. D., 2013, *Applied Mathematics*, 4th ed., John Wiley & Sons, Hoboken, NJ.
- [36] Harris, C. R., Millman, K. J., van der Walt, S. J., Gommers, R., Virtanen, P., Cournapeau, D., Wieser, E., Taylor, J., Berg, S., Smith, N. J., Kern, R., Picus, M., Hoyer, S., van Kerkwijk, M. H., Brett, M., Haldane, A., Fernández del Río, J., Wiebe, M., Peterson, P., Gérard-Marchant, P., Sheppard, K., Reddy, T., Weckesser, W., Abbasi, H., Gohlke, C., and Oliphant, T. E., 2020, "Array Programming With NumPy," *Nature*, **585**(7825), pp. 357–362.
- [37] Virtanen, P., Gommers, R., Oliphant, T. E., Haberland, M., Reddy, T., Cournapeau, D., Burovski, E., Peterson, P., Weckesser, W., Bright, J., van der Walt, S. J., Brett, M., Wilson, J., Millman, K. J., Mayorov, N., Nelson, A. R. J., Jones, E., Kern, R., Larson, E., Carey, C. J., Polat, I., Feng, Y., Moore, E. W., VanderPlas, J., Laxalde, D., Perktold, J., Cimrman, R., Henriksen, I., Quintero, E. A., Harris, C. R., Archibald, A. M., Ribeiro, A. H., Pedregosa, F., van Mulbregt, P., and SciPy 1.0 Contributors, 2020, "SciPy 1.0: Fundamental Algorithms for Scientific Computing in Python," *Nature Methods*, **17**, pp. 261–272.
- [38] IEEE, 2019, "IEEE Standard for Floating-Point Arithmetic, IEEE Std 754TM-2019 (Revision of IEEE Std 754-2008)," doi: [10.1109/IEEESTD.2019.8766229](https://doi.org/10.1109/IEEESTD.2019.8766229).
- [39] Dormand, J. R. and Prince, P. J., 1980, "A Family of Embedded Runge-Kutta Formulae," *Journal of Computational and Applied Mathematics*, **6**(1), pp. 19–26.
- [40] Prince, P. J. and Dormand, J. R., 1981, "High Order Embedded Runge-Kutta Formulae," *Journal of Computational and Applied Mathematics*, **7**(1), pp. 67–75.
- [41] Hairer, E., Nørsett, S. P., and Wanner, G., 1993, *Solving Ordinary Differential Equations I: Nonstiff Problems*, 2nd ed., No. 8 in Springer Series in Computational Mathematics, Springer, Berlin, The Federal Republic of Germany.
- [42] Rohatgi, A., "WebPlotDigitizer," <https://automeris.io>
- [43] Shurman, J., 2016, *Calculus and Analysis in Euclidean Space*, Undergraduate Texts in Mathematics, Springer International Publishing, Cham, The Swiss Confederation.
- [44] Morro, A. and Giorgi, C., 2023, *Mathematical Modelling of Continuum Physics. Modeling and Simulation in Science, Engineering and Technology*, Springer Nature Switzerland AG, Cham, The Swiss Confederation.
- [45] Hertz, H. R., 1881, "Über die Berührung fester elastischer Körper," *Journal für die reine und angewandte, Mathematik*, **92**, pp. 156–171. The reference is based on a translation that was performed using Adobe's PDF to Word conversion tool and <https://stringtranslate.com>.
- [46] Hertz, H. R., 1882, "Über die Berührung fester elastischer Körper und über die Härte," *Verhandlungen des Vereins zur Beförderung des Gewerbefleißes*, Berlin: Verein zur Beförderung des Gewerbefleißes, pp. 449–463. The reference is based on a translation that was performed using Adobe's PDF to Word conversion tool and <https://stringtranslate.com>.
- [47] Popov, V. L., Heß, M., and Willert, E., 2019, *Handbook of Contact Mechanics: Exact Solutions of Axisymmetric Contact Problems*, Springer, Berlin, The Federal Republic of Germany.
- [48] 2025, "Online Materials Information Resource - MatWeb," accessed 2025-07-05, <https://www.matweb.com/>
- [49] Ragonneau, T. M., 2023, "Model-Based Derivative-Free Optimization Methods and Software," doi: [10.48550/arXiv.2210.12018](https://doi.org/10.48550/arXiv.2210.12018), arXiv:2210.12018 [math], <http://arxiv.org/abs/2210.12018>
- [50] Ragonneau, T. M. and Zhang, Z., 2024, "An Optimal Interpolation Set for Model-Based Derivative-Free Optimization Methods," *Optimization Methods and Software*, **39**(4), pp. 898–910.
- [51] Ragonneau, T. M. and Zhang, Z., 2024, "PDFO: A Cross-Platform Package for Powell's Derivative-Free Optimization Solvers," *Mathematical Programming Computation*, **16**(4), pp. 535–559.
- [52] Ruina, A. and Pratap, R., 2019, *Introduction to Mechanics for Engineers*, Rudra Pratap and Andy Ruina.
- [53] Biswas, S. and Chatterjee, A., 2014, "A Reduced-Order Model From High-Dimensional Frictional Hysteresis," *Proceedings of the Royal Society A: Mathematical, Physical and Engineering Sciences*, **470**(2166), p. 20130817.
- [54] Biswas, S. and Chatterjee, A., 2015, "A Two-State Hysteresis Model From High-Dimensional Friction," *Royal Society Open Science*, **2**(7), p. 150188.

- [55] Vaiana, N., Sessa, S., Marmo, F., and Rosati, L., 2018, "A Class of Uniaxial Phenomenological Models for Simulating Hysteretic Phenomena in Rate-Independent Mechanical Systems and Materials," *Nonlinear Dynamics*, **93**(3), pp. 1647–1669.
- [56] Vaiana, N., Sessa, S., and Rosati, L., 2021, "A Generalized Class of Uniaxial Rate-Independent Models for Simulating Asymmetric Mechanical Hysteresis Phenomena," *Mechanical Systems and Signal Processing*, **146**, p. 106984.
- [57] Vaiana, N. and Rosati, L., 2023, "Analytical and Differential Reformulations of the Vaiana–Rosati Model for Complex Rate-Independent Mechanical Hysteresis Phenomena," *Mechanical Systems and Signal Processing*, **199**, p. 110448.
- [58] Vaiana, N. and Rosati, L., 2023, "Classification and Unified Phenomenological Modeling of Complex Uniaxial Rate-Independent Hysteretic Responses," *Mechanical Systems and Signal Processing*, **182**, p. 109539.
- [59] Wolfram Research Inc, 2023, "Mathematica, Version 13.3," <https://www.wolfram.com/mathematica>
- [60] Takeuti, G. and Zaring, W. M., 1982, *Introduction to Axiomatic Set Theory*, 2nd ed., No. 1 in Graduate Texts in Mathematics, Springer-Verlag New York, New York, NY.
- [61] Kelley, J. L., 1955, *General Topology*, Van Nostrand Reinhold Company. Reprint, Dover Publications Inc., 2017., Mineola, NY.
- [62] Bloch, E. D., 2010, *The Real Numbers and Real Analysis*, Springer Science+Business Media, New York, NY.
- [63] Ziemer, W. P. and Torres, M., 2017, *Modern Real Analysis*, 2nd ed., No. 278 in Graduate Texts in Mathematics, Springer International Publishing, Cham, The Swiss Confederation.
- [64] Yoshizawa, T., 1966, *Stability Theory by Liapunov's Second Method*, No. 9 in Publications of the Mathematical Society of Japan, The Mathematical Society of Japan, Tokyo, Japan.
- [65] Yoshizawa, T., 1975, *Stability Theory and the Existence of Periodic Solutions and Almost Periodic Solutions*, No. 14 in Applied Mathematical Sciences, Springer-Verlag New York, New York, NY.
- [66] Sontag, E. D., 1998, *Mathematical Control Theory: Deterministic Finite Dimensional Systems*, 2nd ed., Texts in Applied Mathematics, Springer Science+Business Media, New York, NY.
- [67] Haddad, W. M. and Chellaboina, V., 2011, *Nonlinear Dynamical Systems and Control: A Lyapunov-Based Approach*, Princeton University Press, Princeton, NJ.
- [68] Khalil, H. K., 2015, *Nonlinear Control*, Pearson Education, Upper Saddle River, NJ.